Eur Biophys J (1993) 22:367–378

European Biophysics Journal

Invited Review

Total internal reflection fluorescence microscopy: application to substrate-supported planar membranes

Nancy L. Thompson, Kenneth H. Pearce, Helen V. Hsieh

Department of Chemistry, University of North Carolina, Chapel Hill, NC 27599-3290, USA

Received: 14 July 1993 / Accepted: 16 July 1993

Abstract. The use of total internal reflection illumination in fluorescence microscopy (TIRFM) is reviewed with emphasis on application to fluorescent macromolecules that specifically and reversibly bind to planar model membranes supported on glass or quartz substrates. Several methods for characterizing macromolecular motion and organization are discussed: the measurement of equilibrium binding curves to obtain values for equilibrium binding constants; the measurement of fluorescence photobleaching recovery curves to obtain values of kinetic rate constants and surface diffusion coefficients; and the measurement of fluorescence intensities as a function of the evanescent field polarization to characterize orientational order. Applications to cell-substrate contact regions are summarized and future directions of TIRFM are outlined.

Key words: Evanescent field – Surface diffusion – Receptor-ligand interactions – Fluorescence photobleaching recovery – Fluorescence correlation spectroscopy

Introduction

Defining the structural and dynamic aspects of biochemical processes that occur at cell membrane surfaces is central to understanding a variety of biological phenomena. For example, signal transduction across plasma membranes involves the interaction of external chemical signals from solution, transmembrane receptors, and other membrane-associated proteins such as G proteins; thrombosis and hemostasis require chemistry involving components such as the prothrombinase enzyme complex and integrins that are found on platelet and endothelial cell surfaces; oxidative phosphorylation results from membrane-associated molecular events that occur on the inner mitochondrial membrane; and the synthesis of transmembrane and secretory proteins occurs on endoplasmic reticulum membranes.

One method for examining molecular motion and organization at phospholipid membrane surfaces is to use model membranes constructed on planar transparent surfaces (McConnell et al. 1986; Thompson and Palmer 1988; Tamm and Kalb 1993). A variety of methods have been used or developed for forming supported planar membranes. For example, single phospholipid monolayers or bilayers may be deposited on substrates using the Langmuir-Blodgett method, phospholipid vesicles may be adsorbed to and fused at solid surfaces from adjacent solutions, and phospholipids may be deposited on surfaces by detergent dialysis. Substrate-supported planar membranes are chemically and physically well-defined and are amenable to most surface techniques, such as optical microscopy, ellipsometry, atomic force or other probe microscopies, neutron reflection, and X-ray scattering.

A surface technique that has been particularly useful for probing macromolecular dynamics at supported planar membranes is total internal reflection fluorescence microscopy (TIRFM). In this method, a thin layer ($\approx$1 000 Å) of surface-associated illumination that penetrates into the liquid adjacent to a substrate-supported planar membrane is created by a totally internally reflected light source. This layer of surface-associated light, called the evanescent field, is used to excite fluorescent molecules that are adsorbed to the planar membrane. A variety of techniques in fluorescence microscopy may be combined with evanescent excitation to probe the behavior of the membrane-bound fluorescent molecules. Aspects of total internal reflection fluorescence have been described in a number of recent reviews (Axelrod et al. 1984; Thompson et al. 1988; Hellen et al. 1988; Axelrod 1989; Reichert 1989; Axelrod 1990; Toriumi and Masuhara 1991; Axelrod et al. 1992; Tamm 1993; Thompson et al. 1993). Here, we primarily describe measurements made using fluorescence microscopy (TIRFM) and emphasize applications to the study of proteins at biologically-relevant planar model membranes and to quantitative characterization of cell-substrate contact regions.

Correspondence to: N. L. Thompson

Total internal reflection fluorescence at planar interfaces

The physical aspects of evanescent fields created by total internal reflection at a planar dielectric interface have been described previously (Mahan and Bitterli 1978; Axelrod et al. 1984, 1992). A plane wave travelling through a medium of a higher refractive index n_1 will be completely reflected into this medium if it encounters a planar interface with a medium of lower refractive index n_2 at an incidence angle θ which is greater than the critical angle θ_c, where

$$\theta_c = \sin^{-1}\left(\frac{n_2}{n_1}\right). \tag{1}$$

Although the plane wave is completely reflected at the interface, a surface-associated evanescent electromagnetic field is created in the medium of lower refractive index (Fig. 1). This field propagates parallel to the interface in a direction (denoted as the x-axis) which is the intersection of the incidence and sample planes. The evanescent field has an intensity $I(z)$ which decreases exponentially as a function of the distance z from the interface. Here,

$$I(z) = I_0\, e^{-z/d} \tag{2}$$

where

$$\frac{I_0}{I_i} = \frac{4n_1^2 \cos^2\theta(2n_1^2 \sin^2\theta - n_2^2)}{n_2^4 \cos^2\theta + n_1^4 \sin^2\theta - n_1^2 n_2^2} \quad (p\text{-}polarized) \tag{3}$$

$$\frac{I_0}{I_i} = \frac{4n_1^2 \cos^2\theta}{n_1^2 - n_2^2} \quad (s\text{-}polarized) \tag{4}$$

$$d = \frac{\lambda}{4\pi\sqrt{n_1^2 \sin^2\theta - n_2^2}}. \tag{5}$$

In Eqs. (3–5), λ is the vacuum wavelength and I_i is the intensity of the incident light. Figure 2 shows the values of θ_c, d and I_0/I_i for typical experimental conditions. The manner in which the evanescent wave depth and intensity depend on the incidence angle and on the solution refractive index have been (in part) experimentally verified (Axelrod 1981; Suci and Reichert 1988a, b; Pearce et al. 1992).

The polarization of the evanescent electric field has been described in detail elsewhere (Axelrod et al. 1984; Thompson et al. 1984; Abney et al. 1992) and is illustrated in Fig. 3. When an incident plane wave is *s*-polarized (i.e., is polarized along the y-axis), the direction of the evanescent electric field is parallel to the plane where internal reflection occurs and perpendicular to the evanescent propagation direction. When an incident plane wave is *p*-polarized (i.e., is polarized perpendicular to the propagation direction and within the incidence plane), the direction of the evanescent electric field rotates in time and space through the x-z plane but is polarized primarily along the z-axis. In this case, the evanescent field is not transverse.

Equations (1–5) hold when the incident light is a plane wave. However, experimentally, the incident light is usually a Gausian-shaped laser beam that is roughly focused at the point of internal reflection. The evanescent electric field produced in this experimental case has been examined theoretically (Burghardt and Thompson 1984a). For typical experimental conditions, these calculations predict that the spatial dependence of the evanescent intensity in the interface plane is approximately of an elliptical Gaussian shape, i.e.

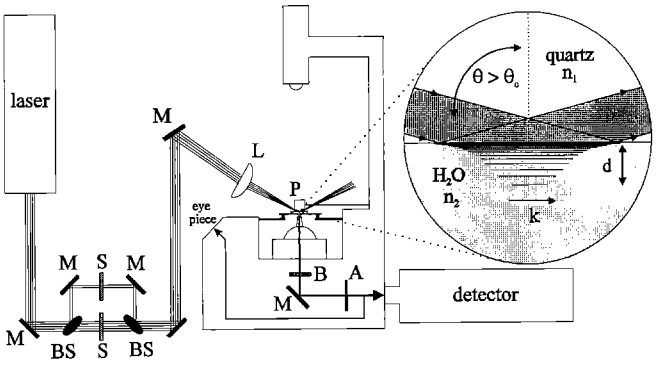

Fig. 1. Schematic diagram of an optical arrangement for a TIRFM apparatus. Shown is the optical configuration used for TIRFM and TIR-FPR. Two 10:90 beam splitters (BS) are used to create beams of relatively high and low intensities. Two shutters (S) are used to control both the bleaching and illumination beams. The laser beam is directed by mirrors (M) and a focussing lens (L) to a fixed quartz prism (P) where the light is incident at an angle θ (which is greater than the critical angle θ_c) on a planar dielectric interface. The totally internally reflected laser beam creates a Gaussian shaped evanescent field with depth, d, and propagation vector, $\boldsymbol{k}$. Fluorescence is directed through a barrier filter (B) and an aperture (A) to a detector

$$I(x,y) \propto \exp\left[-\frac{2x^2}{(\gamma s)^2}\right] \exp\left[-\frac{2y^2}{s^2}\right] \tag{6}$$

where s is the $1/e^2$ radius perpendicular to the direction of propagation, $\gamma > 1$ defines the eccentricity of the ellipse, and these two parameters are determined by optical factors such as the incident beam radius and the presence of auxiliary lenses. Equation (6) has been experimentally confirmed (Fig. 4a). The calculations also predict that the evanescent depth is approximately equal to that shown in Eq. (5) throughout the spatial range of the evanescent field, and that the evanescent field polarization is approximately equivalent to the predicted polarization for an incident plane wave.

Materials present on the interface where total internal reflection occurs may perturb the characteristics of the evanescent field. For example, if a planar slab of material with a refractive index different from n_2 or n_1 is present at the interface, the electromagnetic field at the sample plane may be significantly altered (Palik and Holm 1978; Gingell et al. 1987). If large, nonplanar materials with different refractive indices (such as 10-μm diameter polystyrene beads) are present on the interface, significant scattering and perturbations in the local evanescent field may occur (Lan et al. 1986; Brown et al. 1989; Prieve and Frej 1990). However, scattering and other evanescent wave effects are negligible for very thin uniform films such as phospholipid monolayers or bilayers (Reichert 1989). Absorbing materials may also significantly alter the evanescent field (Toriumi et al. 1992). However, these effects are insignificant for typical fluorophore surface densities (Burghardt and Axelrod 1981). Because the effective pathlength for

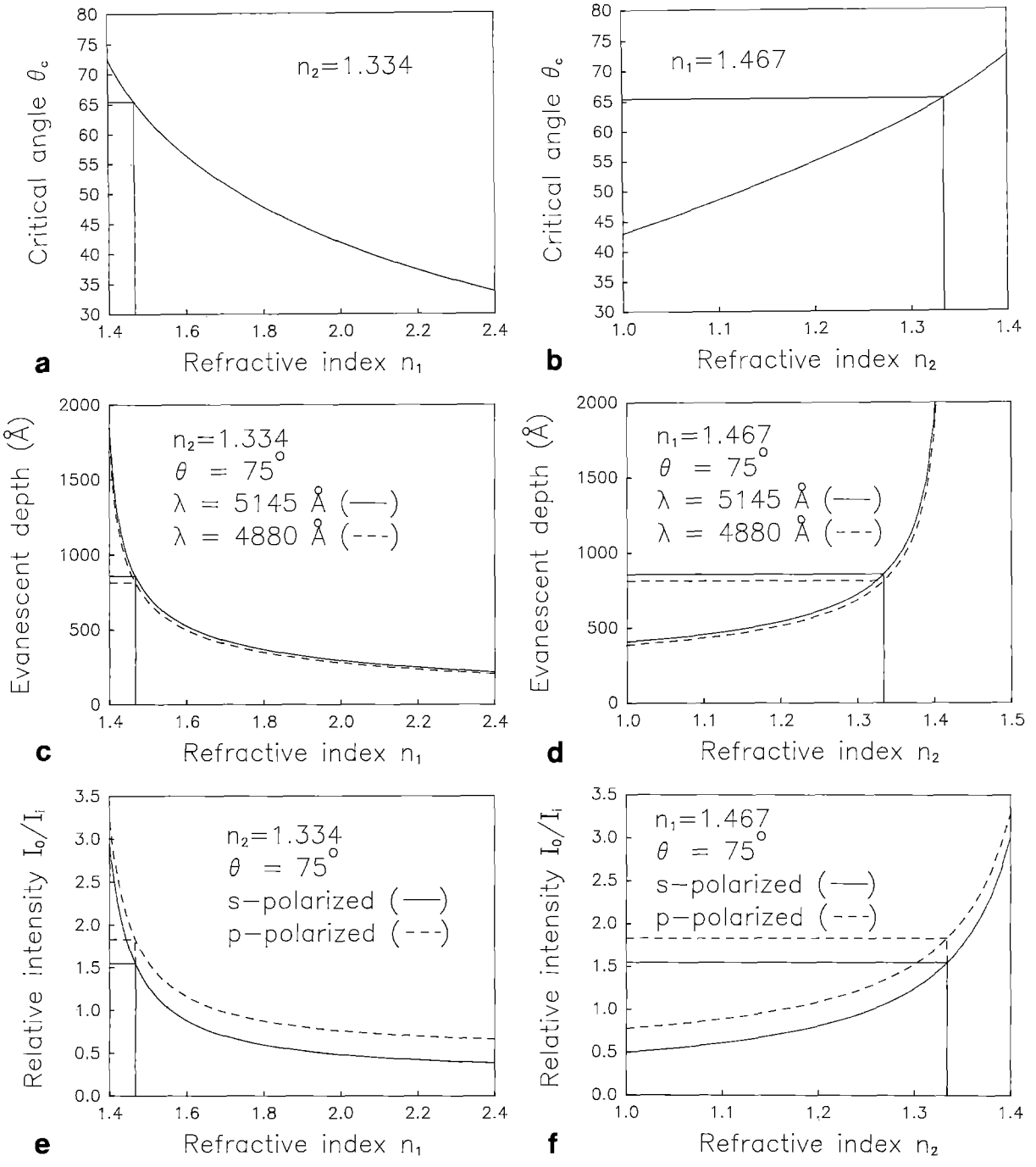

Fig. 2a–f. Theoretical values of the critical angle θ_c, the penetration depth d, and the evanescent intensity I_0/I_i. **a, b** The critical angle θ_c ranges from 35° to 75° for refractive indices near those of quartz ($n_1 = 1.467$) or water ($n_2 = 1.334$). For these values of n_1 and n_2, $\theta_c = 65.4°$. **c, d** For $\theta = 75°$, the penetration depth d is $\approx \lambda$ except for when $n_1 \approx n_2$, where $d \to \infty$. For $n_1 = 1.467$ and $n_2 = 1.334$, $d = 813$ Å (for $\lambda = 4880$ Å) or $d = 857$ Å (for $\lambda = 5145$ Å). **e, f** The evanescent intensity at $z = 0$, I_0, is $\approx I_i$. Although I_0 depends on the polarization of the incident beam, θ_c and d do not. Plots were calculated using Eqs. (1–5)

absorbance is ≈ 0.1 μm (Gingell et al. 1987; Reichert 1989), significant absorption (e.g., $\geq 5\%$) will occur for a solute with a molar absorptivity of 10^4 M^{-1} cm^{-1} only if the concentration is ≥ 0.5 M.

In all measurements that use an evanescent field to excite fluorescence, the probe molecules are very close to a planar dielectric interface. The presence of the discontinuous refractive index dramatically alters the characteristics of the fluorescence emission. The effects of the near-by interface on the fluorescence quantum efficiency, lifetime, and angular emission profile have been considered in depth theoretically (Burghardt and Thompson 1984b; Thompson and Burghardt 1986; Hellen and Axelrod 1987; Axelrod and Hellen 1989; Burghardt 1989). Some of these predicted effects have been experimentally confirmed (Lee et al. 1979; Suci and Reichert 1988a, b). Metal films at the interface can also have significant effects on the properties of the emitted fluorescence (Weber and

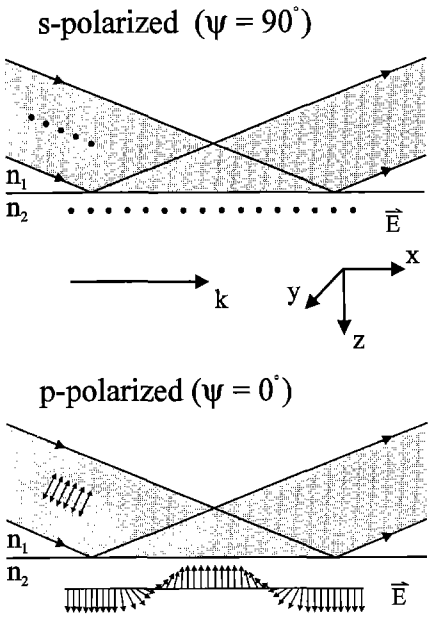

Fig. 3. Evanescent field polarization. The polarization of the incident laser beam, ψ, is defined from the incidence $(x-z)$ plane. (*top*) When $\psi = 90°$ (*s*-polarized), the polarization of the evanescent field is parallel to the interface and perpendicular to the direction of propagation of the evanescent field, $\boldsymbol{k}$. (*bottom*) When $\psi = 0°$ (*p*-polarized), the polarization of the evanescent field is primarily perpendicular to the interface, but also contains a small, nontransverse component that is parallel both to the interface and to the evanescent propagation direction; in this case, the evanescent polarization rotates in time and space through the incidence plane

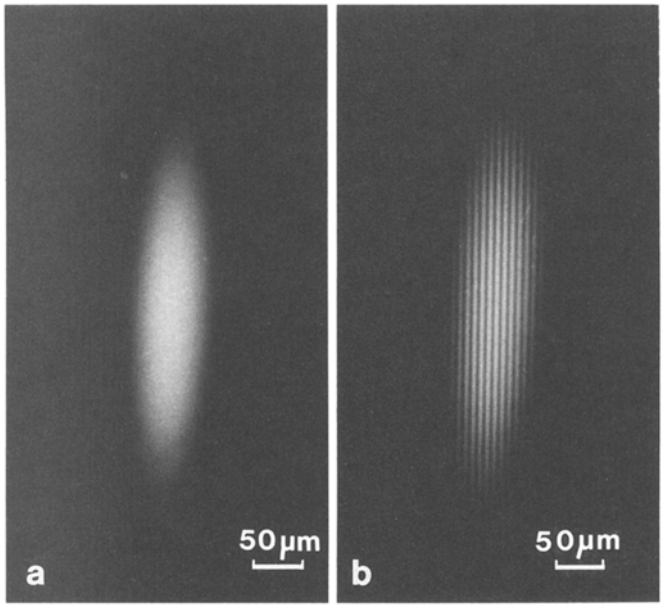

Fig. 4a, b. Experimental evanescent fields. Evanescent fields were created by totally internally reflecting an argon ion laser beam through a quartz prism: **a** single beam; **b** two interfering beams

Eagen 1979; Ford and Weber 1984; Axelrod et al. 1986; Hellen and Axelrod 1987; Aroca et al. 1988). Finally, if the density of fluorescent molecules is too high, self-quenching may occur; however, previous work has shown that the evanescently excited fluorescence is proportional to the fluorophore surface density up to at least 14 000 molecules/μm^2 (Lok et al. 1983a, b).

Numerous instrumental methods for creating evanescent light at a planar interface and for collecting the fluorescence emitted by nearby molecules have been developed for optical microscopes. Comprehensive reviews of different optical designs may be found elsewhere (Axelrod et al. 1984; Axelrod 1989; Liebmann et al. 1991). One common design uses a cubic prism to couple an incident laser beam to a quartz microscope slide; fluorescence is collected by a microscope objective through the lower refractive index medium (Fig. 1; Poglitsch and Thompson 1990; Pisarchick and Thompson 1990). A newer and particularly interesting design, called prismless TIRFM, is one in which the off-axis components of a light source that broadly illuminates a high aperture microscope objective are totally internally reflected back into the objective, which is also used for fluorescence collection (Stout and Axelrod 1989; Hellen and Axelrod 1991). One may also modify a dark-field condenser to generate evanescent light on an optical microscope (Murray and Eshel 1992).

Surface densities

A primary feature of TIRFM is that it may be used to obtain information about molecules that are only weakly bound to a surface, while the molecules are in chemical equilibrium with an adjacent solution. In general, the measured fluorescence arises both from surface-bound fluorophores and from fluorophores in solution. Thus, the evanescently excited fluorescence is

$$F = Q[C + A\,d] \tag{7}$$

where C is the two-dimensional density of surface-bound fluorophores, A is the solution concentration of fluorophores, d is the evanescent wave depth (Eq. (5)), and Q is proportional to the product of the absorptivity, quantum efficiency, and fluorescence collection efficiency and is assumed here to be equivalent for all molecules.

A variety of methods have been used for determining the fraction f of the measured fluorescence that is attributable to surface-bound molecules rather than molecules in solution: (*1*) the fluorescence intensities on surfaces with and without binding sites may be compared (Pisarchick and Thompson 1990; Poglitsch et al. 1991; Hsieh et al. 1992); (*2*) the fluorescence intensities in the presence and absence of chemical agents that block surface binding may be compared (Poglitsch and Thompson 1990; Pearce et al. 1992); (*3*) the fraction of the measured fluorescence that is bleachable (and therefore surface-bound) may be measured (Schmidt et al. 1990; Zimmermann et al. 1990; Pearce et al. 1992; Pisarchick et al. 1992); (*4*) the fluorescence may be measured as a function of the evanescent depth and extrapolated to zero (Thompson and Axelrod 1983); or (*5*) the fluorescence anisotropy may be compared with measured anisotropies for freely diffusing and surface-bound fluorophores (Thompson and Axelrod 1983). With a measured value of f, the known solution concentration and evanescent field depth provide an internal standard that yields an absolute measure of the

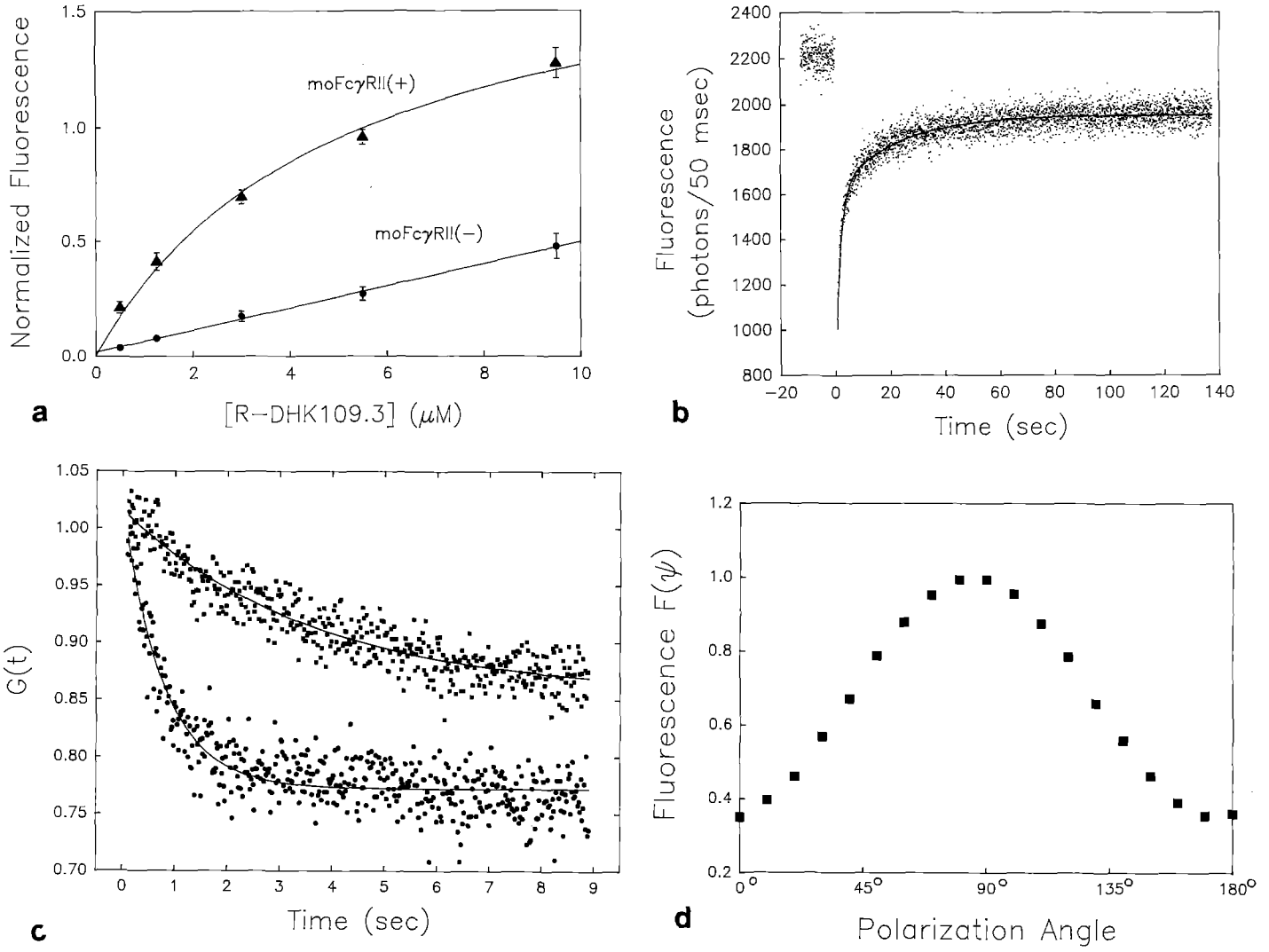

Fig. 5a–d. Examples of experimental data obtained with TIRFM. **a** A tetramethylrhodamine-labelled mouse monoclonal IgG1 antibody (DHK 109.3) specifically associates with supported planar membranes that contain a purified and reconstituted mouse antibody receptor (moFcγRII). TIRFM was used to measure the fluorescence on membranes with and without receptors. The best fit of the difference in fluorescence to Eq. (9) gave $K_d = 2.6$ μM. (Reproduced from Biochem 31:11562 (1992) with copyright permission from the American Chemical Society). **b** A fluorescein-labelled anti-dinitrophenyl mouse monoclonal IgG1 Fab (ANO2) weakly and reversibly binds to supported phospholipid monolayers composed of a mixture of dipalmitoylphosphatidylcholine and dinitrophenylaminocaproyldipalmitoylphosphatidylethanolamine. TIR-FPR was used to obtain intrinsic surface dissociation rates. Shown is a single recovery curve with a sample time of 50 ms. The line shows the best fit to a biexponential form of Eq. (11) and gave two rates with different amplitudes [0.6 s^{-1} (57%) and 0.05 s^{-1} (25%)]. (Reproduced from Biophys J 63:215 (1992) with copyright permission from the Biophysical Society). **c** Nitrobenzoxadiazole-labelled phosphatidylcholine undergoes lateral diffusion in phosphatidylcholine/phosphatidylserine supported phospholipid monolayers. TIR-FPPR was used to examine the diffusion of the labelled phospholipids. Shown are single recovery curves with sample times of 20 ms. The data were obtained with evanescent interference patterns of 6 μm (●, bottom) and 12 μm (■, top). Fluorescence recovery curves were fit to Eq. (16) (with $k_{off} = 0$) and are plotted as $G(t) = [F(-) - F(t)]/[F(-) - F(0)]$ (Huang et al. 1993). **d** The fluorescent lipid dioctadecyltetramethylindocarbocyanine is incorporated into supported phospholipid monolayers composed of distearoylphosphatidylcholine and dinitrophenyldioleoylphosphatidylethanolamine. The fluorescence, measured with P-TIRFM, was maximized when the incident laser beam was *s*-polarized and minimized when the beam was *p*-polarized, indicating that the absorption dipole of the incorporated dye was approximately oriented within the sample plane. (Reproduced from Biophys J 58:413 (1990) with copyright permission from the Biophysical Society)

fluorophore surface density. Here,

$$C = dA\frac{f}{1-f}. \tag{8}$$

Absolute surface densities (C) have also been determined from the extrapolated time-zero value of TIR-FCS autocorrelation functions (Thompson and Axelrod 1983) or from diffusion-limited TIR-FPR recovery curves (Pearce et al. 1992) (see below).

Equilibrium binding curves

A common application of TIRFM is to measure the fluorescence arising from bound molecules as a function of

Table 1. Dissociation constants K_d at planar membranes measured by TIRFM

Fluorescent ligand	Planar membrane	K_d	Site density (molecules/μm²)	References
Insulin	insulin receptor/PC	≤300 pM	–	Sui et al. (1988)
Anti-FcγRII Fab (2.4G2)	macrophage	1 nM	50	Poglitsch and Thompson (1990)
Laminan-nidogen (with Ca^{2+})	PC PG PC/sulfatide	5 nM	1 000	Kalb and Engel (1991)
Anti-FcγRII Fab (2.4G2)	FcγRII/PC/cholesterol	15 nM	1 300	Poglitsch et al. (1991)
Fibrinogen	platelet	40 nM	–	Engel et al. (1992)
Fibrinogen	αIIbβ3/PC/PG	50 nM	–	Müller et al. (1993)
Anti-TNP antibody (GK 14-1)	PC/TNP-PE	20–100 nM	–	Kalb et al. (1990)
Properidin	PC sulfatide	>100 nM	–	Stankowski et al. (1991)
Anti-DNP antibody (ANO2)	PC/DNP-PE	300 nM	6 000	Pisarchick and Thompson (1990)
Bovine prothrombin and its fragment 1 (with Ca^{2+})	PC/PS	1–15 μM	15 000–40 000	Pearce et al. (1992) Pearce et al. (1993)
Polyclonal IgG Monoclonal IgG1	FcγRII/PC/cholesterol	2–3 μM	600	Poglitsch et al. (1991) Hsieh et al. (1992)
Anti-DNP Fab (ANO2)	PC/DNP-PE	2–6 μM	6 000	Pisarchick and Thompson (1990) Pisarchick et al. (1992)
RGD-containing peptide	αIIbβ3/PC/PG	1 μM	–	Müller et al. (1993)
Bovine prothrombin and prethrombin (without Ca^{2+})	PC/PS	> 10 μM	>1 200	Tendian et al. (1991)

Abbreviations: αIIbβ3, integrin; DNP, dinitrophenyl; FcγRII, antibody receptor; PC, phosphatidylcholine; PE, phosphatidylethanolamine; PG, phosphatidylglycerol; PS, phosphatidylserine; TNP, trinitrophenyl

the solution concentration. These measurements may be used to generate an equilibrium binding curve. For a simple bimolecular reaction between monovalent ligands and monovalent surface sites

$$C = \frac{AN}{K_d + A} \tag{9}$$

where K_d is the equilibrium dissociation constant and N is the surface site density at saturation. Thus, the binding curve can yield a value for K_d and, if the fluorescence is calibrated, N (Fig. 5a).

TIRFM has been used to measure the apparent surface dissociation constants for a variety of proteins (antibodies, prothrombin and its proteolytic fragments, fibrinogen, laminan-nidogen, properidin, insulin and RGD-containing peptides) on planar membranes containing a variety of binding site types (hapten-conjugated phospholipids, negatively charged phospholipids, antibody receptors, insulin receptors, integrins) (Table 1). TIRFM has also been used to characterize the adsorption of protein ligands (e.g., bovine serum albumin) to non-biological surfaces (e.g., quartz) (Burghardt and Axelrod 1981; Schmidt et al. 1990; Zimmermann et al. 1990).

Measured K_d values range over more than four orders of magnitude, from 0.3 nM to 15 μM, and have been in good agreement with the values of K_d measured by other methods. The primary limitation of TIRFM at low K_d values is accurately calibrating the solution concentration (Poglitsch and Thompson 1990). For high K_d values, the primary limitation is that the fluorescence arising from specifically bound fluorophores must be a significant fraction of the total collected fluorescence (Tendian et al. 1991). If one assumes that the density of evanescently illuminated, solution-phase fluorophores cannot be greater than the density of surface-bound fluorophores at $A = 3K_d$ and that nonspecific binding is negligible, then the upper limit for measurable dissociation constants is $K_d \leq N/4d$. For $d = 850$ Å, this expression gives $K_d \leq 0.5$ μM for $N = 100$ molecules/μm² and $K_d \leq 50$ μM for $N = 10\,000$ molecules/μm².

Surface binding kinetics

The selective illumination of surface-bound molecules by evanescent illuminaton is advantageous not only for examining the equilibrium aspects of surface binding, but also for directly investigating surface binding kinetics. If the evanescently excited fluorescence is proportional to the surface density of bound, fluorescent molecules (see above), the time-dependence of the fluorescence change following an extrinsic perturbation between bound and unbound states can provide kinetic information about the binding event of interest. Perturbations may be introduced either by creating a chemical change (e.g., a concentration jump) or by changing the spectroscopic properties of the bound state (e.g., irreversible photobleaching).

By using a flow cell adapted for TIRFM, the association kinetics for proteins at planar membrane surfaces may be monitored by introducing fluorescently-labelled ligand, and the dissociation kinetics may be monitored by

Table 2. Association and dissociation kinetic rates at planar membranes measured by TIRFM

Fluorescent ligand	Planar membrane	Notes	k_{off} (s^{-1})	k_{on} ($M^{-1}\,s^{-1}$)	References
Anti-TNP antibody (GK14-1)	PC/TNP-PE	b	1×10^{-4}	1×10^{3}	Kalb et al. (1990)
Fibrinogen	αIIbβ3/PC/PG	b,c	2×10^{-3}	4×10^{4}	Müller et al. (1993)
Epidermal growth factor	A431 human epidermoid cells	a	0.01	2×10^{6}	Hellen and Axelrod (1991)
Polymeric monoclonal IgG1	FcγRII/PC/cholesterol	a	~0.1	–	Hsieh and Thompson (1993 b)
Bovine prothrombin fragment 1	PC/PS	a	0.2	2×10^{4}	Pearce et al. (1992) Pearce et al. (1993)
Bovine prothrombin	PC/PS	a	0.3	5×10^{4}	Pearce et al. (1993)
Anti-DNP Fab (ANO2)	PC/DNP-PE	a	0.5	2×10^{5}	Pisarchick et al. (1992)
Monomeric monoclonal IgG1	FcγRII/PC/cholesterol	a	~1	4×10^{5}	Hsieh and Thompson (1993 b)
Monomeric polyclonal IgG2a	FcγRII/PC/cholesterol	a	~1	–	Hsieh and Thompson (1993 b)
Monomeric monoclonal IgG1	FcγRII/PC/cholesterol	a	~1	–	Hsieh and Thompson (1993 b)

Abbreviations: αIIbβ3, integrin; DNP, dinitrophenyl; FcγRII, antibody receptor; PC, phosphatidylcholine; PE, phosphatidylethanolamine; PG, phosphatidylglycerol; PS, phosphatidylserine; TNP, trinitrophenyl

Notes: (a) the dissociation rates k_{off} were measured by TIR-FPR and the association rates k_{on} were determined using $k_{on}=k_{off}/K_d$; (b) the association and dissociation rates were measured directly with a flow cell; (c) these data are accurate only for early times in that the binding slowly becomes irreversible

subsequently introducing unlabelled ligand. This direct method of monitoring adsorption and desorption has been used to examine the kinetics for several proteins at supported planar membranes (Table 2) and to characterize the fusion of phospholipid vesicles (either containing or not containing reconstituted proteins) with substrate-supported phospholipid membranes (Kalb and Tamm 1992; Kalb et al. 1992).

A related technique for measuring desorption rate constants from surfaces (e.g., supported planar membranes) is total internal reflection – fluorescence photobleaching recovery (TIR-FPR) (Thompson et al. 1981; Burghardt and Axelrod 1981). In TIR-FPR, surface-bound, fluorescent molecules in equilibrium with the surface are photobleached with a brief pulse of intense evanescent illumination; as time proceeds, bleached molecules desorb and are replaced with unbleached molecules from solution or nonilluminated, surrounding surface areas (Fig. 5b).

In theory, a number of physical processes may influence the shapes of TIR-FPR recovery curves (Thompson et al. 1981). For a simple, monovalent binding mechanism and in the absence of surface diffusion, there are three characteristic rates: the intrinsic dissociation rate, k_{off}; a solution diffusion rate normal to the surface, R_N; and a solution diffusion rate parallel to the surface, R_L. The approximate rate of fluorescence recovery is given by

$$k_{obs}=\min[k_{off},\max\{R_L,R_N\}]. \tag{10}$$

If one or both of the transport rates, R_L and R_N, are large enough so that diffusion in solution does not limit the rate of fluorescence recovery, then TIR-FPR data are "reaction-limited" and provide information about the surface dissociation kinetic rate k_{off}. In this limit,

$$F(t)=F(-)[1-B\exp(-k_{off}t)] \tag{11}$$

where $F(t)$ is the fluorescence after the bleaching pulse, $F(-)$ is the prebleach fluorescence, and B is the fractional bleach. When fluorescence recovery is limited solely by diffusion in solution,

$$F(t)=F(-)[1-B\,e^{R_N t}\,\mathrm{erfc}(\sqrt{R_N t})] \tag{12}$$

where

$$R_N=D\left(\frac{A}{C}\right)^2=\frac{D}{N^2}(K_d+A)^2 \tag{13}$$

and D is the solution diffusion coefficient. Although the primary purpose of this technique is to obtain data under reaction-limited conditions and to therefore measure k_{off}, the technique may also be used to find C (Eq. (13)). Theoretical expressions for analysis of TIR-FPR data for surface binding mechanisms that involve more than one binding site type and/or one or more membrane-bound protein conformations have also been developed (Hsieh and Thompson 1993 a).

TIR-FPR has been used to examine the dissociation kinetics of a variety of proteins at substrate-supported planar membranes (Table 2). This method has also been used to investigate the dissociation rate of epidermal growth factor from its receptor on epidermoid cells (Hellen and Axelrod 1991). The original, less biologically significant applications of TIR-FPR were to proteins non-specifically adsorbed to bare or chemically modified quartz (Burghardt and Axelrod 1981; Tilton et al. 1990 a, b; Schmidt et al. 1990).

The dissociation rates measured by TIRFM and TIR-FPR for proteins that interact in a biologically specific manner with supported planar membranes have been, on the average, lower than the dissociation rates measured in other systems. For example, the measured dissociation rate for an anti-dinitrophenyl Fab from dinitrophenylated planar membranes was 100-fold slower than that measured for the same Fab with dinitrophenyl-glycine in solution (Pisarchick et al. 1992) and the dissociation rate for prothrombin from planar membranes was 10-fold

slower than that measured by quasielastic light scattering using small unilamellar phospholipid vesicles (Pearce et al. 1992; Pearce et al. 1993). In that the measured values of K_d at planar membranes are in good agreement with those measured in similar model systems by different techniques, the apparent association kinetic rates, calculated from TIR-FPR data as $k_{on}=k_{off}/K_d$, are considerably lower than previously measured or inferred on-rates.

A striking result from the assembly of presently available TIR-FPR kinetic data is that, for all systems, the reaction-limited TIR-FPR data are not well described by a single exponential shape. These results imply that the association of the proteins with the planar membranes proceeds through a mechanism or mechanisms that are more complex than a discrete, reversible, bimolecular reaction between monovalent ligands and surface sites (Eqs. (9) and (11)) (Thompson et al. 1981). Although the specific reasons for the complex binding behavior are not known at present, there are at least three possible factors that might in general contribute to the underlying reasons: (*1*) heterogeneous binding site types; (*2*) more than one membrane-bound protein species; (*3*) a feature of the general mechanism of extrinsic protein binding to planar membrane surfaces (e.g., crowding, orientational, rebinding, or electrostatic effects).

A technique closely related to TIR-FPR is total internal reflection – fluorescence correlation spectroscopy (TIR-FCS) (Thompson et al. 1981). In this method, fluctuations in the evanescently excited fluorescence that result from fluorescent molecules binding and dissociating from the surface are autocorrelated, and the fluorescence fluctuation autocorrelation function is used to obtain information about the dissociation kinetic rate. TIR-FCS has been experimentally demonstrated only for the nonspecific, reversible adsorption of blood proteins on protein-coated quartz (Thompson and Axelrod 1983).

Surface diffusion of weakly bound ligands

The combination of total internal reflection and fluorescence pattern photobleaching recovery (TIR-FPPR) can provide information about the lateral motions of proteins weakly bound to supported planar membranes. In this method, a periodic evanescent interference pattern is created by colliding two laser beams at the point where they totally internally reflect (Fig. 4 b). The optical characteristics of evanescent interference patterns and the use of these patterns in TIR-FPPR have been theoretically explored in depth (Abney et al. 1992; Huang and Thompson 1993; Huang et al. 1993; Hsieh and Thompson 1993 a). These calculations indicate that the properties of the evanescent interference patterns and the fluorescence recovery curves depend on the intensities, polarizations, and incidence angles of the two incident beams. In the simplest case, the evanescent intensity profile is the product of Eq. (2), Eq. (6), and the following factor

$$I(y) \propto 1 + V\cos\left[\frac{2\pi y}{P}\right] \tag{14}$$

where

$$P = \frac{\lambda}{2n_1 \sin\theta \sin\phi} \tag{15}$$

is the period of the interference pattern; n_1, λ and θ are defined in Eqs. (1–5); ϕ is the semi-angle between the lines of intersection of the two incidence planes and the sample plane; and V is the visibility (or contrast), which depends on both geometrical and optical parameters. For combined surface reaction and diffusion and with V equal to its maximum value of one (Abney et al. 1992; Huang and Thompson 1993)

$$F(t) = F(-)\left[1 - \exp(-k_{off}t) \cdot \left\{1 - e^{-\eta} I_0(\eta) + e^{-\eta} I_1(\eta) \exp\left(-\frac{4\pi^2 D t}{P^2}\right)\right\}\right] \tag{16}$$

where I_0 and I_1 are modified Bessel functions and η describes the fractional bleach.

The first application of TIR-FPPR was to anti-hapten IgE antibodies in the contact region between rat basophil leukemia cells, which contain Fcε receptors, and substrate-supported phosphatidylcholine monolayers containing hapten-conjugated phosphatidylethanolamine (Weis et al. 1982). The principal use of the patterned evanescent illumination in this work was to control for fluorescence caused by scattered evanescent light. Recently, TIR-FPPR has been used to measure the surface diffusion coefficient of bovine serum albumin absorbed to poly(methylmethacrylate)-coated glass (Tilton et al. 1990 a). By measuring the fluorescence recovery rates as a function of evanescent pattern period, it was shown that tightly-bound proteins underwent translational diffusion with a coefficient $\approx 10^{-9}$ cm^2/s. An accompanying work showed that the protein surface diffusion was reduced at higher protein surface densities (Tilton et al. 1990 b). TIR-FPPR has also been used to monitor the lateral diffusion of fluorescent lipid analogs in supported planar membranes (Fig. 5 c) (Huang et al. 1993). In one study, fluorescent lipid diffusion was monitored during the fusion of phospholipid vesicles with supported planar membranes (Kalb et al. 1992). Recently, TIR-FPPR has been used to measure the translational diffusion of prothrombin fragment 1 weakly and reversibly bound to negatively-charged planar membranes. Preliminary results suggest that the fragment 1 diffuses at $\approx 10^{-9}$ cm^2/s and that the diffusion coefficient decreases with increasing surface density (Huang et al. 1993).

For tightly bound proteins ($k_{off} \to 0$), the maximum post-bleach fluorescence change relative to the prebleach fluorescence, which occurs for $\eta \approx 1.5$ (Eq. (16)), is 0.22. The low signal-to-noise ratio that results from this small change is a major limitation in this method and makes extraction of lateral diffusion information difficult. For loosely bound proteins where the fluorescence recovery also results from association and dissociation kinetics, data analysis is even more difficult. However, a recent and promising theoretical work has suggested that this limitation might be lifted by the use of two-photon excitation, which gives a sharper bleaching and observation profile (Huang and Thompson 1993).

Molecular orientations

Evanescent illumination may also be used to gain information about the orientation distribution of a population of fluorophore absorption dipoles at or near an interface (P-TIRFM) (Thompson et al. 1984). Here, one measures absorption dichroism by examining the dependence of the evanescently excited fluorescence on the polarization of the evanescent field. As the polarization of the incident laser beam is rotated through the plane normal to its direction of propagation, the polarization of the evanescent field rotates (primarily) about the direction of propagation of the evanescent field (Fig. 3). The polarization of the evanescent field therefore probes the polar angle (with respect to the normal to the interface) of the absorption dipoles. The use of polarized evanescent excitation is thus particularly applicable to interfacial samples because, in most of these samples, the orientational anisotropy is found primarily in the polar rather than the azimuthal angle relative to the normal to the interface.

The simplest version of this experimental method is one in which the emitted fluorescence is collected with a very high aperture microscope objective placed on the less dense (aqueous) side of the interface (Thompson et al. 1984). The high aperture insures that the fluorescence collection efficiency is approximately equivalent for fluorophores with different orientations. Therefore, the polarization dependence of the measured fluorescence depends primarily on the absorption dichroism rather than the emission dichroism. Experimental arrangements that reflect emission dichroism are more complicated because one must consider differential fluorescence collection efficiencies. For high aperture collection and for an azimuthally symmetric sample (averaged over the size of the illuminated area), the normalized fluorescence $F(\psi)$ is approximately equal to

$$F(\psi) = 1 + Z[\cos^2\psi - \cos^2\psi_0] \tag{17}$$

where ψ is the polarization angle of the incident beam, ψ_0 is the angle at which $F(\psi)$ is a maximum and equals 0° or 90°, and Z is a constant that contains information about the orientation distribution of absorption dipoles (and also depends on optical parameters). A measure of $F(\psi)$ yields a value for the constant Z. The constant Z may then be related either to an assumed functional form for the angular distribution (model-dependent analysis) or to the moments of the angular orientation distribution of fluorophore absorption dipoles expanded in a series of Legendre polynomials, or "order parameters" (model-independent analysis).

The use of P-TIRFM to examine the orientation distribution of fluorophores at planar dielectric interfaces has a variety of applications: (*1*) When these measurements are made on fluorescent molecules in supported planar membranes, the results may be used to confirm the existence of long-range order in the samples and therefore to provide evidence for membrane integrity. This use of P-TIRFM has been experimentally demonstrated on several sample types, including fluorescent lipids and lipid-peptide conjugates in phospholipid Langmuir-Blodgett films (Fig. 5d) (Thompson et al. 1984; Timbs and Thompson 1990). (*2*) This technique may be used to monitor changes in fluorophore orientation distributions that occur in response to environmental changes. In one previous work, changes in the orientation of a fluorescently tagged phospholipid in a phospholipid Langmuir-Blodgett film were detected as a function of the lipid density (Thompson et al. 1984). In a separate work, changes in the orientation of surface-adsorbed cytochrome *c* were detected as a function of the surface electric potential upon adsorption (Fraaije et al. 1990). (*3*) Orientational information may allow more thorough interpretation of energy transfer measurements, which can provide information about conformational changes that occur upon adsorption (Burghardt and Axelrod 1983) or other parameters that report molecular structure at interfaces. (*4*) Orientational measurements give crucial information for interpreting dynamic fluorescence polarization data that can provide information about molecular rotational mobility and/or segmental flexibility at interfaces (Timbs and Thompson 1990, 1993).

Cell-substrate contact regions

In one of the earliest applications of TIRFM, it was demonstrated that evanescent excitation could be used to selectively visualize cell-substrate contact regions (Axelrod 1981). Subsequently, evanescent excitation has been used to examine the arrangement of a variety of fluorescent probes specific for different membrane components in cell-substrate contact regions. Applications have included visualization of fluorescent reporters bound to cytoskeletal elements in rat myotube membranes that are adjacent to glass substrates (Bloch et al. 1989); fluorescent, hapten-specific IgE antibodies in the regions of contact between rat basophil leukemia cells containing IgE receptors and supported planar membranes containing haptenated phospholipids (Weis et al. 1982); fluorescent peptide antigens and histocompatibility antigens in the regions of contact between antigen-specific helper T cells and supported planar membranes (Watts et al. 1986); fluorescently labelled angiotensin-converting enzyme on endothelial cells that were grown on quartz coated with extracellular matrix components (Nakache et al. 1986); and fluorescent markers in the membranes of mammalian fibroblasts on glass substrates (Lanni et al. 1985). A mathematical basis for mapping the three dimensional topography of fluorescent membrane markers in regions of cell-substrate contact has subsequently been developed (Reichert and Truskey 1990).

In a related version of TIRFM used to examine cell-substrate contact regions, fluorescent molecules reside in the aqueous solution between a cell membrane and a surface to which the cell is attached. If the cell-to-substrate distance is large, the fluorescence is intense; if the distance is small, the fluorescence is weak. Quantitatively measuring the spatial distribution of fluorescence intensities then provides a two-dimensional map of cell-to-substrate contact distances. An extensive theory describing data analysis has been presented (Gingell et al. 1987; Heavens 1990; Reichert and Truskey 1990) and the meth-

od has been applied to chick heart explants (Gingell et al. 1985), *Dictyostelium* amoebae (Todd et al. 1988), and bovine aortic endothelial cells (Truskey et al. 1992) on glass substrates.

There are a few examples of the use of evanescent illumination to probe the dynamics (as opposed to the organization) of fluorescent molecules in cell-substrate contact regions. In the earliest demonstration of this approach, TIR-FPPR was used to probe the lateral mobility of fluorescent antibodies which specifically linked rat basophil leukemia cells to supported planar membranes (Weis et al. 1982). Recently, TIR-FPR has been used to characterize the kinetics of epidermal growth factor binding to its receptor on mildly fixed A431 human epidermoid cells (Hellen and Axelrod 1991). Fluorescent epidermal growth factor in the cell-substrate contact area was illuminated with an evanescent field, and experimental conditions were adjusted so that, after photobleaching, fluorescence recovery gave information about the intrinsic ligand-receptor binding kinetics.

Related developments and future applications

The experimental uses of evanescent illumination are broad, including applications in surface science, analytical chemistry, biochemistry, biophysics, cell biology, biosensors and bioengineering. In this review, we have discussed the use of evanescent illumination with fluorescence microscopy to monitor the motion and organization of proteins reversibly bound to planar membranes deposited on glass or quartz or of macromolecules in the regions of contact between cells and planar substrates.

There are several areas in which one might expect increased further development in TIRFM methodology: (*1*) Imaging methods that use low-light video detectors or charge-coupled devices will be particularly useful for examining cell-substrate contact regions and spatially heterogeneous surfaces (Hlady et al. 1990; Hlady 1991; Truskey et al. 1992). (*2*) Materials other than silicon dioxide may be used to alter the interfacial characteristics and thus optimize or emphasize chosen spectroscopic properties. For example, thin metal or semiconducting films may be used to quench fluorescent molecules that are very close to the membrane-solution interface and to thus enhance the signal from molecules close to but not bound to the interface (Nakache et al. 1986; Axelrod et al. 1986). Transparent media with very high refractive indices, such as sapphire or diamond, may be used to generate extremely thin evanescent fields and to specifically observe only those molecules on or very near the surface (Gigola and Haller 1990; Masuhara 1992). (*3*) Evanescent illumination may be used to examine fluorescence energy transfer between donors and acceptors that are conjugated to molecules weakly bound to surfaces. This method has previously been used to characterize conformational changes that occur in bovine serum albumin upon adsorption to fused silica (Burghardt and Axelrod 1983), to provide evidence for the formation of a monolayer of fluorophores at a decalin/water interface (Morrison and Weber 1987), and to investigate the effects of bound *T* cells on the distance between antigenic peptides and histocompatibility proteins (Watts et al. 1986). (*4*) The use of evanescent illumination with pulsed lasers for probing fluorescence lifetimes and time-resolved anisotropies of fluorophores close to or bound to planar surfaces has recently been used to probe nonbiological systems (Rainbow et al. 1987; Itaya et al. 1990; Fukumara and Hayashi 1990; Rumbles et al. 1991; Toriumi and Masuhara 1991) and is likely to find future application in biophysics.

Acknowledgements. We thank Z. Huang for permission to include his unpublished results (Fig. 5c). This work was supported by National Institutes of Health grant GM-37145 (NLT), by National Science Foundation Grant DMB-9024028, by a Graduate Fellowship from the Hercules Corporation (KHP) and by a Department of Education Graduate Fellowship (HVH).

References

Abney JR, Scalettar BA, Thompson NL (1992) Evanescent interference patterns for fluorescence microscopy. Biophys J 61:542–552

Aroca R, Kovacs GJ, Jennings CA, Loutfy RO, Vincett PS (1988) Fluorescence enhancement from Langmuir-Blodgett monolayers on silver island films. Langmuir 4:518–521

Axelrod D (1981) Cell-substrate contacts illuminated by total internal reflection fluorescence. J Cell Biol 89:141–145

Axelrod D (1989) Total internal reflection fluorescence microscopy. Methods Cell Biol 30:245–270

Axelrod D (1990) Total internal reflection fluorescence at biological surfaces. In: Noninvasive Techniques in Cell Biology. Wiley-Liss, New York, pp 93–127

Axelrod D, Hellen EH (1989) Emission of fluorescence at interfaces. Methods Cell Biol 30:399–416

Axelrod D, Burghardt TP, Thompson NL (1984) Total internal reflection fluorescence. Ann Rev Biophys Bioeng 13:247–268

Axelrod D, Fulbright RM, Hellen EH (1986) Adsorption kinetics on biological membranes: measurement by total internal reflection fluorescence. In: Applications of Fluorescence in the Biomedical Sciences, Alan R Liss: 461–476

Axelrod D, Hellen EH, Fulbright RM (1992) Total internal reflection fluorescence. In: Lakowicz JR (ed) Topics in Fluorescence Spectroscopy, Vol. 3. Plenum Press, New York, pp 289–343

Bloch RJ, Velez M, Krikorian JG, Axelrod D (1989) Microfilaments and actin-associated proteins at sites of membrane-substrate attachment within acetylcholine receptor clusters. Exp Cell Res 182:583–596

Brown MA, Smith AL, Staples EJ (1989) A method using total internal reflection microscopy and radiation pressure to study weak interaction forces of particles near surfaces. Langmuir 5:1319–1324

Burghardt TP (1989) Polarized fluorescence emission from probes near dielectric interfaces. Chem Phys Lipids 50:271–287

Burghardt TP, Axelrod D (1981) Total internal reflection/fluorescence photobleaching recovery study of serum albumin adsorption dynamics. Biophys J 33:455–468

Burghardt TP, Axelrod D (1983) Total internal reflection fluorescence study of energy transfer in surface-adsorbed and dissolved bovine serum albumin. Biochemistry 22:979–985

Burghardt TP, Thompson NL (1984a) Evanescent intensity of a focused Gaussian light beam undergoing total internal reflection in a prism. Opt Eng 23:62–67

Burghardt TP, Thompson NL (1984b) Effect of planar dielectric interfaces on fluorescence emission and detection: Evanescent excitation with high aperture observation. Biophys J 46:729–737

Engel M, Pisarchick ML, Thompson NL, Erickson BW (1992) Binding of a coiled-coil protein to planar platelet membranes by

fluorescence microscopy. In: Smith JA, Rivier JE (ed) Peptides: Chemistry and Biology, ESCOM, Leiden: 464–465
Ford GW, Weber WH (1984) Electromagnetic interactions of molecules with metal surfaces. Phys Rep 113:195–287
Fraaije JGEM, Kleijn JM, van der Graaf M, Dijt JC (1990) Orientation of adsorbed cytochrome *c* as a function of the electric potential of the interface studied by total internal reflection fluorescence. Biophys J 57:965–975
Fukumara H, Hayashi K (1990) Time-resolved fluorescence anisotropy of labeled plasma proteins adsorbed on polymer surfaces. J Coll Int Sci 135:435–442
Gigola CE, Haller GL (1990) A diamond internal reflection cell for infrared measurements on metal and metal oxide films. Appl Spectrosc 44:159–162
Gingell D, Todd I, Bailey J (1985) Topography of cell-glass apposition revealed by total internal reflection fluorescence of volume markers. J Cell Biol 100:1334–1338
Gingell D, Heavens OS, Mellor JS (1987) General electromagnetic theory of total internal reflection fluorescence: the quantitative basis for mapping cell-substratum topography. J Cell Sci 87:677–693
Heavens OS (1990) Cell studies of total internal reflection fluorescence: effect of lipid membranes. J Cell Sci 95:175–176
Hellen EH, Axelrod D (1987) Fluorescence emission at dielectric and metal-film interfaces. J Opt Soc Am B 4:337–350
Hellen EH, Axelrod D (1991) Kinetics of epidermal growth factor/receptor binding on cells measured by total internal reflection/fluorescence recovery after photobleaching. J Fluorescence 1:113–128
Hellen EH, Fulbright RM, Axelrod D (1988) Total internal reflection fluorescence: Theory and applications at biosurfaces. In: Loew LM (ed) Spectroscopic Membrane Probes, Vol. II. CRC Press, Boca Raton, pp 47–58
Hlady V (1991) Spatially resolved adsorption kinetics of immunoglobulin *G* onto the wettability gradient surface. Appl Spectrosc 45:246–252
Hlady V, Lin JN, Andrade JD (1990) Spatially resolved detection of antibody-antigen reaction on solid/liquid interface using total internal reflection excited antigen fluorescence and charge-coupled device detection. Biosens Bioelectr 5:291–301
Hsieh HV, Thompson NL (1993a) Theory for measuring surface binding kinetics using total internal reflection with fluorescence photobleaching recovery. Biophys J (in press)
Hsieh HV, Thompson NL (1993b) Surface binding kinetics between a mouse Fc receptor (moFcγRII) and IgG: a study using total internal reflection with fluorescence photobleaching recovery. (in preparation)
Hsieh HV, Poglitsch CL, Thompson NL (1992) Direct measurement of the weak interactions between mouse Fc receptor (FcγRII) and IgG1 in the absence and presence of hapten: a total internal reflection fluorescence microscopy study. Biochemistry 31:11562–11566
Huang Z, Thompson NL (1993) Theory for two photon excitation in pattern photobleaching with evanescent illumination. Biophys Chem (in press)
Huang Z, Pearce KH, Thompson NL (1993) Translational diffusion of fluorescent lipids and fluorescently-labelled bovine prothrombin fragment 1 associated with substrate-supported planar membranes (in preparation)
Itaya A, Yamada T, Tokuda K, Masuhara H (1990) Interfacial characteristics of poly(methyl methacrylate) film: aggregation of pyrene and micropolarity revealed by time-resolved total internal reflection fluorescence spectroscopy. Polymer J 22:697–704
Kalb E, Engel J (1991) Binding and calcium-induced aggregation of laminin onto lipid bilayers. J Biol Chem 266:19047–19052
Kalb E, Tamm LK (1992) Incorporation of cytochrome b_5 into supported phospholipid bilayers by vesicle fusion to supported monolayers. Thin Solid Films 210/211:763–765
Kalb E, Engel J, Tamm LK (1990) Binding of proteins to specific target sites in membranes measured by total internal reflection fluorescence microscopy. Biochemistry 29:1607–1613
Kalb E, Frey S, Tamm LK (1992) Formation of supported planar bilayers by fusion of vesicles to supported phospholipid monolayers. Biochim Biophys Acta 1103:307–316
Lan KH, Ostrowsky N, Sornette D (1986) Brownian dynamics close to a wall studied by photon correlation spectroscopy from an evanescent wave. Phys Rev Lett 57:17–20
Lanni F, Waggoner AS, Taylor DL (1985) Structural organization of interphase 3T3 fibroblasts studied by total internal reflection fluorescence microscopy. J Cell Biol 100:1091–1102
Lee E, Benner RE, Fenn JB, Chang RK (1979) Angular distribution of fluorescence from liquids and monodispersed spheres by evanescent wave excitation. Appl Opt 18:862–868
Liebmann LW, Robinson JA, Mann KG (1991) A dual beam total internal reflection fluorescence spectrometer for dynamic depth resolved measurements of biochemical liquid-solid interface binding reactions in opaque solvents. Rev Sci Instrum 62:2083–2092
Lok BK, Cheng Y, Robertson CR (1983a) Total internal reflection fluorescence: a technique for examining interactions of macromolecules with solid surfaces. J Colloid Interface Sci 91:87–103
Lok BK, Cheng Y, Robertson CR (1983b) Protein adsorption on crosslinked polydimethylsiloxane using total internal reflection fluorescence. J Colloid Interface Sci 91:104–116
Mahan AI, Bitterli CV (1978) Total internal reflection: a deeper look. Appl Opt 17:509–519
Masuhara H (1992) Space- and time-resolved laser spectroscopy and photochemistry of organic solids. J Photochem Photobiol A Chem 62:397–413
McConnell HM, Watts TH, Weis RM, Brian AA (1986) Supported planar membranes in studies of cell-cell recognition in the immune system. Biochim Biophys Acta 864:95–106
Morrison LE, Weber G (1987) Biological membrane modeling with a liquid/liquid interface: probing mobility and environment with total internal reflection excited fluorescence. Biophys J 52:367–379
Müller B, Zerwes H-G, Tangemann K, Paeter J, Engel J (1993) Two-step binding mechanism of fibrinogen αIIbβ3 integrin reconstituted into planar lipid bilayers. J Biol Chem 268:6800–6808
Murray JM, Eshel D (1992) Evanescent wave microscopy: a simple optical configuration. J Micro 167:49–62
Nakache M, Gaub HE, Schreiber AB, McConnell HM (1986) Topological and modulated distribution of surface markers on endothelial cells. Proc Natl Acad Sci, USA 83:2874–2878
Palik ED, Holm RT (1978) Internal reflection spectroscopy studies of thin films and surfaces. Opt Eng 17:512–524
Pearce KH, Hiskey RG, Thompson NL (1992) Surface binding kinetics of prothrombin fragment 1 on planar membranes measured by total internal reflection fluorescence microscopy. Biochemistry 31:5983–5995
Pearce KH, Hof M, Lentz BR, Thompson NL (1993) Comparison of the membrane binding kinetics of bovine prothrombin and its fragment 1. J Biol Chem (in press)
Pisarchick ML, Thompson NL (1990) Binding of a monoclonal antibody and its Fab fragment to supported phospholipid monolayers measured by total internal reflection fluorescence microscopy. Biophys J 58:1235–1249
Pisarchick ML, Gesty D, Thompson NL (1992) Binding kinetics of an anti-dinitrophenyl monoclonal Fab on supported phospholipid monolayers measured by total internal reflection with fluorescence photobleaching recovery. Biophys J 63:215–223
Poglitsch CL, Thompson NL (1990) Interaction of antibodies with Fc receptors in substrate-supported planar membranes measured by total internal reflection fluorescence microscopy. Biochemistry 29:248–254
Poglitsch CL, Sumner MT, Thompson NL (1991) Binding of IgG to moFcγRII purified and reconstituted into supported planar membranes as measured by total internal reflection fluorescence microscopy. Biochemistry 30:6662–6671
Prieve DC, Frej NA (1990) Total internal reflection microscopy: a quantitative tool for the measurement of colloidal forces. Langmuir 6:396–403

Rainbow MR, Atherton S, Eberhart RC (1987) Fluorescence lifetime measurements using total internal reflection fluorimetry: evidence for a conformational change in albumin adsorbed to quartz. J Biomed Mat Res 21:539–555

Reichert WM (1989) Evanescent detection of adsorbed films: Assessment of optical considerations for absorbance and fluorescence spectroscopy at the crystal/solution and polymer/solution interfaces. Crit Rev Biocomp 5:173–205

Reichert WM, Truskey, GA (1990) Total internal reflection fluorescence (TIRF) microscopy. I. Modelling cell contact region fluorescence. J Cell Sci 96:219–230

Rumbles G, Brown AJ, Phillips D (1991) Time-resolved evanescent wave induced fluorescence spectroscopy. J Chem Soc Faraday Trans 87:825–830

Schmidt CF, Zimmermann RM, Gaub HE (1990) Multilayer adsorption of lysozyme on a hydrophobic substrate. Biophys J 57:577–588

Stankowski S, Wey J, Kalb E, Goundis D (1991) Membrane interaction of 'peptide P' derived from the repeating motif of properdin. Biochem Biophys Acta 1068:61–67

Stout AL, Axelrod D (1989) Evanescent field excitation of fluorescence by epi illumination microscopy. Appl Opt 28:5237–5242

Suci PA, Reichert WM (1988a) Demonstration of reciprocity in the angular pattern of fluorescence emission collected from Langmuir-Blodgett deposited thin films. Appl Spectrosc 42:120–127

Suci PA, Reichert WM (1988b) Determination of fluorescence density profiles of Langmuir-Blodgett deposited films by analysis of variable-angle fluorescence data curves. Langmuir 4:1131–1141

Sui S, Urumow T, Sackmann E (1988) Interaction of insulin receptors with lipid bilayers and specific and nonspecific binding of insulin to supported membranes. Biochemistry 27:7463–7469

Tamm LK (1993) Total internal reflectance fluorescence microscopy. In: Optical Microscopy: Emerging Methods and Applications. Academic Press, New York, pp 295–337

Tamm LK, Kalb E (1993) Microspectrofluorometry on supported planar membranes. In: Molecular Luminescence Spectroscopy: Methods and Applications, Part 3. Wiley, New York, pp 253–305

Tendian SW, Lentz BR, Thompson NL (1991) Evidence from total internal reflection fluorescence microscopy for calcium-independent binding of prothrombin to negatively charged planar membranes. Biochemistry 30:10991–10999

Thompson NL, Axelrod D (1983) Immunoglobulin surface binding kinetics studied by total internal reflection with fluorescence correlation spectroscopy. Biophys J 43:103–114

Thompson NL, Burghardt TP (1986) Total internal reflection fluorescence: measurement of spatial and orientational distributions of fluorophores near planar dielectric interfaces. Biophys Chem 25:91–97

Thompson NL, Palmer AG (1988) Model cell membranes on planar substrates. Comments Mol Cell Biophys 5:39–56

Thompson NL, Burghardt TP, Axelrod D (1981) Measuring surface dynamics of biomolecules by total internal reflection fluorescence with photobleaching recovery or correlation spectroscopy. Biophys J 33:435–454

Thompson NL, McConnell HM, Burghardt TP (1984) Order in supported phospholipid monolayers detected by the dichroism of fluorescence excited by polarized evanescent illumination. Biophys J 46:739–747

Thompson NL, Palmer AG, Wright LL, Scarborough PE (1988) Fluorescence techniques for supported planar model membranes. Comments Mol Cell Biophys 5:109–131

Thompson NL, Poglitsch CL, Timbs MM, Pisarchick ML (1993) Dynamics of antibodies on planar model membranes. Acct Chem Res (in press)

Tilton RD, Robertson CR, Gast AP (1990a) Lateral diffusion of bovine serum albumin adsorbed at the solid-liquid interface. J Colloid Interface Sci 137:192–203

Tilton RD, Gast AP, Robertson CR (1990b) Surface diffusion of interacting proteins: effect of concentration on the lateral mobility of adsorbed bovine serum albumin. Biophys J 58:1321–1326

Timbs MM, Thompson NL (1990) Slow rotational mobilities of antibodies and lipids associated with substrate-supported phospholipid monolayers as measured by polarized fluorescence photobleaching recovery. Biophys J 58:413–428

Timbs MM, Thompson NL (1993) Measurement of restricted rotational diffusion of fluorescent lipids in supported planar phospholipid monolayers using angle-dependent polarized fluorescence photobleaching recovery. Biopolymers 33:45–57

Todd I, Mellor JS, Gingell D (1988) Mapping cell-glass contacts of *Dictyostelium* amoebae by total internal reflection aqueous fluorescence overcomes a basic ambiguity of interference reflection microscopy. J Cell Sci 89:107–114

Toriumi M, Masuhara H (1991) Time-resolved total internal reflection fluorescence spectroscopy: principles, instruments, and applications. Spectrochim Acta Rev 14:353–377

Toriumi M, Yanagimachi M, Masuhara H (1992) Absorption effects on total internal reflection fluorescence spectroscopy. Appl Opt 31:6376–6382

Truskey GA, Burmeister JS, Grapa E, Reichert WM (1992) Total internal reflection fluorescence microscopy (TIRFM). II. Topographical mapping of relative cell/substratum separation distances. J Cell Sci 103:491–499

Watts TH, Gaub HE, McConnell HM (1986) T-cell-mediated association of peptide antigen and major histocompatibility complex protein detected by energy transfer in an evanescent wave-field. Nature 320:176–179

Weber WH, Eagen CF (1979) Energy transfer from an excited dye molecule to the surface plasmons of an adjancent metal. Opt Lett 4:236–238

Weis RM, Balakrishnan K, Smith BA, McConnell HM (1982) Stimulation of fluorescence in a small contact region between rat basophil leukemia cells and planar lipid membrane targets by coherent evanescent radiation. J Biol Chem 257:6440–6445

Zimmermann RM, Schmidt CF, Gaub HE (1990) Absolute quantities and equilibrium kinetics of macromolecular adsorption measured by fluorescence photobleaching in total internal reflection. J Colloid Interface Sci 139:268–280